Available online at www.sciencedirect.com

ScienceDirect

IFAC Papers Online CONFERENCE PAPER ARCHIVE

IFAC PapersOnLine 50-1 (2017) 4869–4874

Mixed H_2/H_∞ Tracking Control with Constraints for Single Quadcopter Carrying a Cable-suspended Payload

Minhuan Guo * **Yan Su** ** **Dongbing Gu** ***

* *Nanjing University of Science and Technology, Nanjing, 210094, China (e-mail: 312012201@njust.edu.cn).*
** *Nanjing University of Science and Technology, Nanjing, 210094, China (suyan@njust.edu.cn).*
*** *School of Computer Science and Electronic Engineering, University of Essex, Wivenhoe Park, Colchester, CO4 3SQ, UK, (e-mail: dgu@essex.ac.uk)*

Abstract: In order to control a single quadcopter with a cable-suspended payload to follow the desired trajectory, a mixed H_2/H_∞ controller with constraints is developed. Firstly, the Euler-Lagrange dynamic model is built and linearized. Then the extended model for path tracking problem is designed. Based on linear matrix inequality (LMI), state feedback controller H_2 and H_∞ with constraints is illustrated. Aiming to maintain a good balance in transient behaviors and frequency-domain performance, the mixed controller is presented. Finally, the control strategies are utilized in a simulation test and the result validates the proposed method.

Keywords: aircraft control, H_2 norm, H_∞ norm, linear matrix inequality, Lyapunov function, state control.

1. INTRODUCTION

Nowadays unmanned aerial vehicles (UAVs) are gaining more and more popularity in many possible applications including search and rescue, disaster relief operations, environmental monitoring, wireless surveillance networks, and cooperative manipulation. Lifting and transportation of a cable-suspended payload by a quadcopter is a challenging and useful issue.

Much literature has been published around this topic. Cruz and Fierro (2014) addresses the problem of lifting from the ground a cable-suspended load by a quadrotor aerial vehicle, where the mass of the load is unknown. Faust et al. (2013) presents a motion planning method for generating trajectories with minimal residual oscillations for rotorcraft carrying a suspended load and completes the multi-waypoint flight in the cluttered environment. Palunko et al. (2012) uses a high-level planner to provide desired waypoints and utilize a dynamic programming approach to generate the swing-free trajectory to keep the minimum load swing. Sreenath et al. (2013) establishes a differentially-flat hybrid system for the quadrotor-load system and develops a nonlinear geometric controller to enable tracking of outputs. As for the controller design, in De Crousaz et al. (2014), the iLQG method is applied to the hybrid system and the aggressive controller is designed for controlling the payload to pass through a small window. Alothman et al. (2015) proposes a linear quadratic regulator (LQR) for lifting and transporting the load. The single situation is extended to multi-vehicles in Sreenath and Kumar (2013), which addresses the problem of cooperative transportation of a cable-suspended payload by multiple quadcopters.

This paper presents a mixed H_2/H_∞ tracking controller based on linear matrix inequality (LMI). Basically, problems around H_2 and H_∞ control are studied widely. Apkarian et al. (2001), Zhai et al. (2003), and Filasova et al. (2016) describe the framework for H_2 and H_∞ performance based on linear matrix inequality. It is known that while H_∞ control design is mainly concerned with frequency-domain performance, and does not guarantee good transient behaviors for the closed-loop system, H_2 control design gives more suitable performance on system transient behaviors Nonami and Sivrioglu (1996). The proposed method tries to maintain a good balance on transient behavior and frequency-domain performance. Besides, the constraints for the inputs and outputs are also considered in this paper.

The remaining parts of this paper are organized as follows. In section 2, the nonlinear and linear models are described. In section 3, the extended model for tracking problem is given and the mixed H_2/H_∞ controller is presented. In section 4, the proposed method is developed in a simulation test and the results are analyzed. Finally, a brief conclusion is provided.

2. MODEL DESCRIPTION

2.1 System and Notations

The full system is presented in Fig. 1, including the inertial frame, intermediate frame, body-fixed frame, thrust and torques with respect to the body frame and swing angles

10.1016/j.ifacol.2017.08.976

of the rope with respect to the intermediate frame.
In order to simplify the problem, some reasonable hypotheses are given as follows:

(1) The quadcopter is considered as a geometrical symmetrical rigid body.
(2) The payload is considered as a point mass and is attached at the center of the quadcopter.
(3) The cable tension is always non-zero.
(4) The air drag of the propellers is negligible.

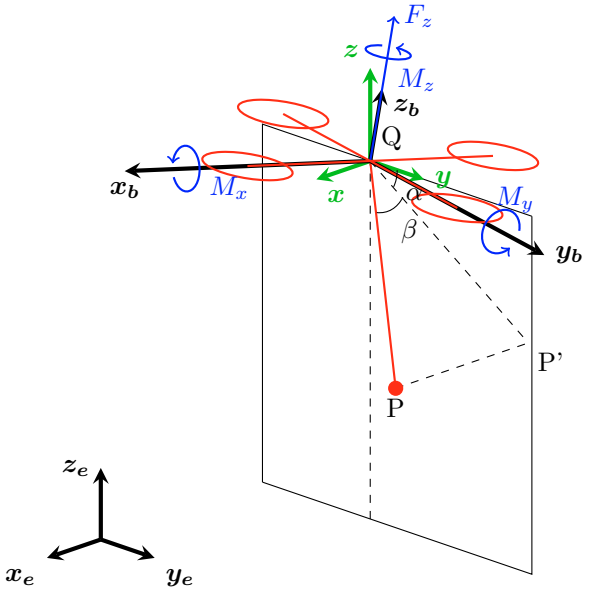

Fig. 1. Single quadcopter with a cable-suspended payload

Partial symbols and acronyms used in this paper are lised in table 1.

Table 1. Symbols and Definitions

Symbol	Description
$\boldsymbol{S_e}: \boldsymbol{x_e y_e z_e}$	Inertial frame
$\boldsymbol{S}: \boldsymbol{xyz}$	Intermediate frame: translate $\boldsymbol{S_e}$ to the center of the quadcopter
$\boldsymbol{S_b}: \boldsymbol{x_b y_b z_b}$	Body-fixed frame
$\boldsymbol{E}_i \in \mathbb{R}^3, i = 1,2,3$	Unit orthogonal vectors of $\boldsymbol{S_e}$
$\boldsymbol{e}_i \in \mathbb{R}^3, i = 1,2,3$	Unit orthogonal vectors of $\boldsymbol{S_b}$
$\boldsymbol{\eta} = [\phi, \theta, \psi]^T \in \mathbb{R}^3$	Euler angles of quadcopter defined in $Z-Y-X$
$\boldsymbol{T}_{e2b} \in \mathbb{R}^{3\times3}$	Transformation matrix from $\boldsymbol{S_e}$ to $\boldsymbol{S_b}$
$\boldsymbol{\Omega} \in \mathbb{R}^3$	Angular velocity of quadcopter in $\boldsymbol{S_b}$
$m_Q = 0.55kg$	Mass of the quadcopter
$m_P = 0.05kg$	Mass of the payload
$\boldsymbol{I}_Q = [I_x, I_y, I_z] \in \mathbb{R}^3$	Inertial matrix of the quadcopter with respect to $\boldsymbol{S_b}$
$\boldsymbol{\xi}_Q \in \mathbb{R}^3$	Position of the center of copter in $\boldsymbol{S_e}$
$\boldsymbol{\xi}_P \in \mathbb{R}^3$	Position of the payload in $\boldsymbol{S_e}$
$L_r = 0.5m$	Length of the rope
$\alpha, \beta \in \mathbb{R}$	Angles of the rope with respect to $\boldsymbol{S}$
$\boldsymbol{\rho} \in \mathbb{R}^3$	Unit vector from the payload to the attached point
$\boldsymbol{F_Q} = [0, 0, F_z]^T$	Forces generated by propellers in $\boldsymbol{S_b}$
$\boldsymbol{M_Q} = [M_x, M_y, M_z]^T$	Torques generated by propellers in $\boldsymbol{S_b}$

As illustrated in Fig. 1, the following relationships are available.

$$\begin{aligned} \boldsymbol{\rho} &= [-sin(\beta), -cos(\alpha)cos(\beta), sin(\alpha)cos(\beta)]^T \\ \boldsymbol{\xi}_P &= x_P\boldsymbol{E_1} + y_P\boldsymbol{E_2} + z_P\boldsymbol{E_3} \\ \boldsymbol{\xi}_Q &= \boldsymbol{\xi}_P + L_r\boldsymbol{\rho} \end{aligned} \tag{1}$$

The rotational velocity Jacobian is

$$\boldsymbol{\Omega} = \boldsymbol{J}\dot{\boldsymbol{\eta}} = \begin{bmatrix} 1 & 0 & -sin(\theta) \\ 0 & cos(\phi) & sin(\phi)cos(\theta) \\ 0 & -sin(\phi) & cos(\phi)cos(\theta) \end{bmatrix} \begin{bmatrix} \dot{\phi} \\ \dot{\theta} \\ \dot{\psi} \end{bmatrix} \tag{2}$$

2.2 Euler-Lagrange Modeling

The quadcopter-payload system has 8 degrees of freedom. Choosing $\boldsymbol{q} = [x_P, y_P, z_P, \alpha, \beta, \phi, \theta, \psi]^T$ as the generalized coordinates will not only be convenient while controlling the trajectory of the payload but also be helpful for extending to multi-vehicle situation. As a result, the Lagrangian is given by

$$\begin{aligned} T &= \frac{1}{2}m_P\dot{\boldsymbol{\xi}}_P^T \cdot \dot{\boldsymbol{\xi}}_P + \frac{1}{2}m_Q\dot{\boldsymbol{\xi}}_Q^T \cdot \dot{\boldsymbol{\xi}}_Q + \frac{1}{2}\boldsymbol{\Omega}^T\boldsymbol{I}_Q\boldsymbol{\Omega} \\ U &= m_P g\boldsymbol{\xi}_P \cdot \boldsymbol{E}_3 + m_Q g\boldsymbol{\xi}_Q \cdot \boldsymbol{E}_3 \\ L &= T - U \end{aligned} \tag{3}$$

Then the Euler-Lagrange equation is

$$\frac{d}{\mathrm{d}t}\left(\frac{\partial L}{\partial \dot{\boldsymbol{q}}}\right) - \frac{\partial L}{\partial \boldsymbol{q}} = \boldsymbol{Q} \tag{4}$$

The generalized forces $\boldsymbol{Q}$ defined here are based on the choice of the generalized coordinates $\boldsymbol{q}$ and the external conservative forces $\boldsymbol{F} = \left[\boldsymbol{F_Q^T}, \boldsymbol{M_Q^T}\right]^T$.

As $\boldsymbol{M_Q}$ is not defined based on Euler angle, a transformation from $\boldsymbol{M_Q}$ to its generalized form in terms of Euler angles is $\boldsymbol{M_\eta} = [M_\phi, M_\theta, M_\psi]^T$

$$\boldsymbol{M_\eta} = \boldsymbol{J}^T\boldsymbol{M_Q} \tag{5}$$

according the powerflow through the joint

$$\boldsymbol{M_\eta} \cdot \dot{\boldsymbol{\eta}} = \boldsymbol{M_\eta^T}\dot{\boldsymbol{\eta}} = \left(\boldsymbol{J}^T\boldsymbol{M_Q}\right)^T\dot{\boldsymbol{\eta}} = \boldsymbol{M_Q} \cdot \dot{\boldsymbol{\Omega}}$$

As a result of D'Alembert's Principle, the generalized force $\boldsymbol{Q}$ is given by equation (6).

$$Q_i = \boldsymbol{F_Q} \cdot \frac{\partial \boldsymbol{\xi}_Q}{\partial q_i} + \boldsymbol{M_\eta} \cdot \frac{\partial \boldsymbol{\eta}}{\partial q_i}, i = 1, 2, ...8 \tag{6}$$

Taking the generalized forces (detailed in (A.1)) and equation (3) into equation (4), the Euler-Lagrange equation can be rewritten in

$$\boldsymbol{G}\ddot{\boldsymbol{q}} = g(\boldsymbol{F}, \boldsymbol{q}, \dot{\boldsymbol{q}}) = f(\boldsymbol{x}, \boldsymbol{u}) \tag{7}$$

where, $\boldsymbol{G}$ and $f(\boldsymbol{x}, \boldsymbol{u})$ are detailed in (A.2) and (A.3) respectively, $\boldsymbol{u} = [F_z, M_x, M_y, M_z]^T \in \mathbb{R}^4$, $\boldsymbol{x} = \left[x_P, \dot{x}_P, y_P, \dot{y}_P, z_P, \dot{z}_P, \alpha, \dot{\alpha}, \beta, \dot{\beta}, \phi, \dot{\phi}, \theta, \dot{\theta}, \psi, \dot{\psi}\right]^T \in \mathbb{R}^{16}$.

Considering the balance situation as the equilibrium point ($\boldsymbol{F}_0$,$\boldsymbol{q}_0$,$\dot{\boldsymbol{q}}_0$) or ($\boldsymbol{x}_0$,$\boldsymbol{u}_0$), the linearized model is obtained in equation (8).

$$\boldsymbol{G}\ddot{\boldsymbol{q}} = f(\boldsymbol{x}_0, \boldsymbol{u}_0) + \left.\frac{\partial f}{\partial \boldsymbol{x}}\right|_{(\boldsymbol{x}_0,\boldsymbol{u}_0)} \delta\boldsymbol{x} + \left.\frac{\partial f}{\partial \boldsymbol{u}}\right|_{(\boldsymbol{x}_0,\boldsymbol{u}_0)} \delta\boldsymbol{u} \quad (8)$$

where, $\delta\boldsymbol{x} = \boldsymbol{x} - \boldsymbol{x}_0$, $\delta\boldsymbol{u} = \boldsymbol{u} - \boldsymbol{u}_0$, $\delta\boldsymbol{q} = \boldsymbol{q} - \boldsymbol{q}_0$, $\boldsymbol{G}\ddot{\boldsymbol{q}}_0 = f(\boldsymbol{x}_0, \boldsymbol{u}_0)$.

Furthermore, the second-order differential equation (8) can be stated in the following standard state-space form.

$$\begin{aligned} \Delta\dot{\boldsymbol{x}} &= \boldsymbol{A}\Delta\boldsymbol{x} + \boldsymbol{B}\Delta\boldsymbol{u} \\ \Delta\boldsymbol{y} &= \boldsymbol{C}\Delta\boldsymbol{x} \end{aligned} \quad (9)$$

where $\boldsymbol{A} \in \mathbb{R}^{16\times16}$ and $\boldsymbol{B} \in \mathbb{R}^{16\times4}$ are detailed in (A.4) and (A.5), $\boldsymbol{C} = \boldsymbol{I}^{16\times16}$.

3. CONTROL STRATEGIES

3.1 Extended Model for Tracking Path

Taking account of the integrations of the position tracking error, the diagram of state feedback controller is seen in Fig. 2.

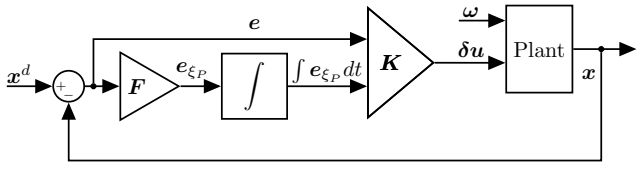

Fig. 2. Diagram of extended state feedback controller

The desired trajectory is $(\boldsymbol{x}^d, \boldsymbol{u}^d)$ and the state tracking error is $\boldsymbol{e} \in \mathbb{R}^{16} := \boldsymbol{x}^d - \boldsymbol{x}$. Specifically, the position tracking error is $\boldsymbol{e}_{\xi_P} \in \mathbb{R}^3 := \left[x_P^d - x_P, y_P^d - y_P, z_P^d - z_P\right]^T$ and its integration is $\int \boldsymbol{e}_{\xi_P} dt$.

The new error state is $\bar{\boldsymbol{e}} = \left[\boldsymbol{e}^T, \int \boldsymbol{e}_{\xi_P}^T dt\right]^T \in \mathbb{R}^{19}$.

Therefore, equation (9) can be stated in following form of tracking error $\bar{\boldsymbol{e}}$ and disturbance inputs $\boldsymbol{\omega} \in \mathbb{R}^4$.

$$\begin{bmatrix} \dot{\boldsymbol{e}} \\ \boldsymbol{e}_{\xi_P} \end{bmatrix} = \bar{\boldsymbol{A}} \begin{bmatrix} \boldsymbol{e} \\ \int \boldsymbol{e}_{\xi_P} dt \end{bmatrix} + \boldsymbol{B}_\omega\boldsymbol{\omega} + \boldsymbol{B}_u\delta\boldsymbol{u} \quad (10)$$

where, $\bar{\boldsymbol{A}} = \left[\begin{array}{c|c} \boldsymbol{A} & \boldsymbol{0} \\ \hline \boldsymbol{F} & \boldsymbol{0} \end{array}\right] \in \mathbb{R}^{19\times19}$, $\boldsymbol{B}_\omega = \boldsymbol{B}_u = \begin{bmatrix} \boldsymbol{B} \\ \boldsymbol{0} \end{bmatrix} \in \mathbb{R}^{19\times4}, \boldsymbol{F} = \boldsymbol{0}^{3\times16}\,(except\ for\ \boldsymbol{F}_{11,23,35} = 1)\,, \delta\boldsymbol{u} = (\boldsymbol{u}^d - \boldsymbol{u})$. The new error state $\bar{\boldsymbol{e}}$ is detectable and considered as the measurement output. The H_2, H_∞ and constraint performance outputs are as follows:

$$\begin{aligned} \boldsymbol{z}_2 &= \boldsymbol{C}_2\bar{\boldsymbol{e}} + \boldsymbol{D}_2\delta\boldsymbol{u} \\ \boldsymbol{z}_\infty &= \boldsymbol{C}_\infty\bar{\boldsymbol{e}} + \boldsymbol{D}_\infty\delta\boldsymbol{u} \\ \boldsymbol{z}_c &= \boldsymbol{C}_c\bar{\boldsymbol{e}} + \boldsymbol{D}_c\delta\boldsymbol{u} \end{aligned} \quad (11)$$

where $\boldsymbol{C}_2$, $\boldsymbol{D}_2$, $\boldsymbol{C}_\infty$, $\boldsymbol{D}_\infty$, $\boldsymbol{C}_c$, $\boldsymbol{D}_c$ are appropriate weight matrix.

As a result, the dynamic model in equation (10) and (11) can be restated using compact notation. Further more, it can be described as a transfer matrix $\boldsymbol{G}$ from disturbances and control inputs to H_2 and H_∞ performances.

$$\begin{aligned} \begin{bmatrix} \dot{\bar{\boldsymbol{e}}} \\ \hline \boldsymbol{z}_2 \\ \boldsymbol{z}_\infty \end{bmatrix} &= \left[\begin{array}{c|cc} \bar{\boldsymbol{A}} & \boldsymbol{B}_w & \boldsymbol{B}_u \\ \hline \boldsymbol{C}_2 & 0 & \boldsymbol{D}_2 \\ \boldsymbol{C}_\infty & 0 & \boldsymbol{D}_\infty \end{array}\right] \begin{bmatrix} \bar{\boldsymbol{e}} \\ \hline \boldsymbol{\omega} \\ \delta\boldsymbol{u} \end{bmatrix} \\ \Rightarrow \boldsymbol{G} &= \begin{bmatrix} \boldsymbol{G}_{11} & \boldsymbol{G}_{12} \\ \boldsymbol{G}_{21} & \boldsymbol{G}_{22} \end{bmatrix} \end{aligned} \quad (12)$$

The proposed controller is to find a feedback gain matrix $\boldsymbol{K}_{mix}$,

$$\delta\boldsymbol{u} = \boldsymbol{K}_{mix}\bar{\boldsymbol{e}} \quad (13)$$

Then, the closed loop control system is

$$\dot{\bar{\boldsymbol{e}}} = \left(\bar{\boldsymbol{A}} + \boldsymbol{B}_u\boldsymbol{K}_{mix}\right)\bar{\boldsymbol{e}} + \boldsymbol{B}_\omega\boldsymbol{\omega} \quad (14)$$

The problem of the mixed H_2/H_∞ tracking control with constraints is described as follows:

$$\begin{aligned} &\min_{K_{mix}} \left\|\boldsymbol{T}_{\boldsymbol{z}_2\to\boldsymbol{\omega}}(\boldsymbol{K}_{mix})\right\|_2 \\ &s.t. \left\|\boldsymbol{T}_{\boldsymbol{z}_\infty\to\boldsymbol{\omega}}(\boldsymbol{K}_{mix})\right\|_\infty \le \gamma \\ &\left|\boldsymbol{u}_i(t)\right| \le u_{i\max} \\ &\left|\boldsymbol{z}_{ci}(t)\right| \le z_{i\max} \end{aligned} \quad (15)$$

where, $\boldsymbol{T}_{\boldsymbol{z}_2\to\boldsymbol{\omega}}(\boldsymbol{K}_{mix})$ denotes the closed transfer function from $\boldsymbol{\omega}$ to $\boldsymbol{z}_2$, $\boldsymbol{T}_{\boldsymbol{z}_\infty\to\boldsymbol{\omega}}$ denotes the closed transfer function from $\boldsymbol{\omega}$ to $\boldsymbol{z}_\infty$, γ is the acceptable gain of H_∞ norm, $u_{i\max}$ and $z_{i\max}$ are the constraints.

3.2 Mixed H_2/H_∞ LMI Control with Constraints

Lemma 1. (Optimal H_2 Control)
If there exist symmetric positive definite matrices $\boldsymbol{X}_2$, $\boldsymbol{Z}$ and general matrix $\boldsymbol{R}_2$ satisfying

$$\begin{aligned} &\min\lambda \\ &s.t. \boldsymbol{X}_2 = \boldsymbol{X}_2^T \succ 0, \boldsymbol{Z} = \boldsymbol{Z}^T \succ 0 \\ &\begin{bmatrix} \boldsymbol{A}\boldsymbol{X}_2 + \boldsymbol{X}_2\boldsymbol{A}^T + \boldsymbol{B}_u\boldsymbol{R}_2 + \boldsymbol{R}_2^T\boldsymbol{B}_u^T * & \\ \boldsymbol{B}_\omega^T & -\boldsymbol{I} \end{bmatrix} \prec 0 \\ &\begin{bmatrix} \boldsymbol{Z} & * \\ \boldsymbol{X}_2\boldsymbol{C}_2^T + \boldsymbol{R}_2^T\boldsymbol{D}_2^T & \boldsymbol{X}_2 \end{bmatrix} \succ 0 \\ &tr\boldsymbol{Z} < \lambda^2 \end{aligned} \quad (16)$$

where state-feedback gain matrix $\boldsymbol{K}_2 = \boldsymbol{R}_2\boldsymbol{X}_2^{-1}$. Then, the controller stabilizes the closed-loop system and the optimal upper bound of H_2 performance index is λ. Hereafter, $*$ denotes the symmetric item in a symmetric matrix.

Proof. See Apkarian et al. (2001).

Lemma 2. (H_∞ Control with Constraints)
Given an upper bound $\gamma > 0$, if there exit symmetric positive definite matrix $\boldsymbol{Q}_\infty$, positive diagonal matrix $\boldsymbol{U}, \boldsymbol{Y}$ and general matrix $\boldsymbol{Y}_\infty$ satisfying

$$
\begin{aligned}
\boldsymbol{Q}_\infty = \boldsymbol{Q}_\infty^T \succ 0 \\
\begin{bmatrix} \boldsymbol{A}\boldsymbol{Q}_\infty + \boldsymbol{Q}_\infty\boldsymbol{A}^T + \boldsymbol{B}_u\boldsymbol{Y}_\infty + \boldsymbol{Y}_\infty^T\boldsymbol{B}_u^T & * & * \\ \boldsymbol{C}_\infty\boldsymbol{Q}_\infty + \boldsymbol{D}_\infty\boldsymbol{Y}_\infty & -\gamma\boldsymbol{I} & * \\ \boldsymbol{B}_w^T & \boldsymbol{0} & -\gamma\boldsymbol{I} \end{bmatrix} \prec 0 \\
\begin{bmatrix} \frac{1}{\alpha}\boldsymbol{U} & \boldsymbol{Y}_\infty \\ * & \boldsymbol{Q}_\infty \end{bmatrix} \succ 0, \boldsymbol{U}_{ii} \prec u_{imax}^2 \\
\begin{bmatrix} \frac{1}{\alpha}\boldsymbol{Y} & \boldsymbol{C}_c\boldsymbol{Q}_\infty + \boldsymbol{D}_c\boldsymbol{Y}_\infty \\ * & \boldsymbol{Q}_\infty \end{bmatrix} \succ 0, \boldsymbol{Y}_{ii} \prec z_{imax}^2
\end{aligned} \tag{17}
$$

where, α is some appropriate constant and state-feedback gain matrix $\boldsymbol{K}_\infty = \boldsymbol{Y}_\infty\boldsymbol{Q}_\infty^{-1}$. Then, the controller meets the constraints, robustly stabilizes the closed-loop system and the upper bound of H_∞ performance index is γ.

Proof. The proof for H_∞ is seen in Filasova et al. (2016). Since $\boldsymbol{K}_\infty = \boldsymbol{Y}_\infty\boldsymbol{Q}_\infty^{-1}$ is the state feedback gain for H_∞ performance, it guarantees the closed system $\boldsymbol{A} + \boldsymbol{B}_u\boldsymbol{K}_\infty$ to be asymptotic stable.
Choosing $V(\boldsymbol{x}(t)) = ||\boldsymbol{Q}_\infty^{-1/2}\boldsymbol{x}(t)||_2^2$ as the Lyapunov function, we get

$$
\frac{d}{dt}V(\boldsymbol{x}(t)) + \gamma^{-1}\|\boldsymbol{z}_\infty(t)\|^2 - \gamma\|\boldsymbol{w}(t)\|^2 \leq 0 \tag{18}
$$

As $\frac{d}{dt}V(\boldsymbol{x}(t)) \leq 0$ and $\frac{\|\boldsymbol{z}_\infty(t)\|^2}{\|\boldsymbol{w}(t)\|^2} \leq \gamma^2$. After integration, we get

$$
V(\boldsymbol{x}(t)) + \gamma^{-1}\int_0^t \|\boldsymbol{z}_\infty(\tau)\|^2 d\tau \leq \gamma\int_0^t \|\boldsymbol{w}(\tau)\|^2 d\tau + V(\boldsymbol{x}(0)) \tag{19}
$$

Assume $\int_0^\infty \|\boldsymbol{w}(t)\|^2 dt \leq w_{\max}$, equation (19) means the state $\boldsymbol{x}$ stays in the ellipsoid:

$$
\Omega(\boldsymbol{Q}_\infty^{-1/2}, \alpha) = \{\boldsymbol{x} \in \mathbb{R}^n | V(\boldsymbol{x}) \leq \alpha\} \tag{20}
$$

where, $\alpha = \gamma w_{\max} + V(\boldsymbol{x}(0))$.
Constraints for the inputs and outputs are:

$$
\begin{aligned}
\max_{t\geq 0}|\boldsymbol{u}_i(t)|^2 &= \max|(\boldsymbol{Y}_\infty\boldsymbol{Q}_\infty^{-1})_i\boldsymbol{x}(t)|^2 \\
&\leq \max_{\boldsymbol{x}\in\Omega}|(\boldsymbol{Y}_\infty\boldsymbol{Q}_\infty^{-1})_i\boldsymbol{x}|^2 \\
&\leq \alpha||(\boldsymbol{Y}_\infty\boldsymbol{Q}_\infty^{-\frac{1}{2}})_i||_2^2 \\
\max_{t\geq 0}|\boldsymbol{z}_{ci}(t)|^2 &= \max|(\boldsymbol{C}_c + \boldsymbol{D}_c\boldsymbol{Y}_\infty\boldsymbol{Q}_\infty^{-1})_i\boldsymbol{x}(t)|^2 \\
&\leq \max_{\boldsymbol{x}\in\Omega}|(\boldsymbol{C}_c + \boldsymbol{D}_c\boldsymbol{Y}_\infty\boldsymbol{Q}_\infty^{-1})_i\boldsymbol{x}|^2 \\
&\leq \alpha||((\boldsymbol{C}_c\boldsymbol{Q}_\infty + \boldsymbol{D}_c\boldsymbol{Y}_\infty)\boldsymbol{Q}_\infty^{-\frac{1}{2}})_i||_2^2
\end{aligned} \tag{21}
$$

where, subscript i means the ith row of the matrix.
Finally, equation (21) can be rewritten in the forms in equation (17). This concludes the proof.

Lemma 3. (H_2/H_∞ Control Synthesis with Constraints) Given γ as upper bound of H_∞, if there exist symmetric positive definite matrices $\boldsymbol{X}$, $\boldsymbol{Z}$, positive diagonal matrix $\boldsymbol{U}, \boldsymbol{Y}$ and general matrix $\boldsymbol{R}$ satisfying

$$
\begin{aligned}
\min\lambda \\
s.t. \boldsymbol{X} = \boldsymbol{X}^T \succ 0, \boldsymbol{Z} = \boldsymbol{Z}^T \succ 0 \\
tr\boldsymbol{Z} < \lambda^2 \\
\begin{bmatrix} \boldsymbol{Z} & * \\ \boldsymbol{X}\boldsymbol{C}_2^T + \boldsymbol{R}^T\boldsymbol{D}_2^T & \boldsymbol{X} \end{bmatrix} \succ 0 \\
\begin{bmatrix} \boldsymbol{A}\boldsymbol{X} + \boldsymbol{X}\boldsymbol{A}^T + \boldsymbol{B}_u\boldsymbol{R} + \boldsymbol{R}^T\boldsymbol{B}_u^T & * \\ \boldsymbol{B}_u^T & -\boldsymbol{I} \end{bmatrix} \prec 0 \\
\begin{bmatrix} \boldsymbol{A}\boldsymbol{X} + \boldsymbol{X}\boldsymbol{A}^T + \boldsymbol{B}_u\boldsymbol{R} + \boldsymbol{R}^T\boldsymbol{B}_u^T & * & * \\ \boldsymbol{C}_\infty\boldsymbol{X} + \boldsymbol{D}_\infty\boldsymbol{R} & -\gamma\boldsymbol{I} & * \\ \boldsymbol{B}_w^T & \boldsymbol{0} & -\gamma\boldsymbol{I} \end{bmatrix} \prec 0 \\
\begin{bmatrix} \frac{1}{\alpha}\boldsymbol{U} & \boldsymbol{R} \\ * & \boldsymbol{X} \end{bmatrix} \succ 0, \boldsymbol{U}_{ii} \prec u_{imax}^2 \\
\begin{bmatrix} \frac{1}{\alpha}\boldsymbol{Y} & \boldsymbol{C}_c\boldsymbol{X} + \boldsymbol{D}_c\boldsymbol{R} \\ * & \boldsymbol{X} \end{bmatrix} \succ 0, \boldsymbol{Y}_{ii} \prec z_{imax}^2
\end{aligned} \tag{22}
$$

where state-feedback gain matrix $\boldsymbol{K}_{mix} = \boldsymbol{R}\boldsymbol{X}^{-1}$. Then, the controller meets the constraints and the H_∞ performance index γ. Meanwhile, the optimal upper bound of H_2 performance index is λ.

Proof. Considering that $\boldsymbol{K}_2$ and $\boldsymbol{K}_\infty$ in Lemma 1 and 2 should be consistent, after enforcing $\boldsymbol{X} = \boldsymbol{X}_2 = \boldsymbol{Q}_\infty$ and $\boldsymbol{R} = \boldsymbol{R}_2 = \boldsymbol{Y}_\infty$, equation (22) is obtained.

4. SIMULATION RESULTS

In order to check the effectiveness of the proposed controller, a simulation test has been implemented on Matlab/Simulink. From 1s the designed controller starts to carry the payload from the initial position $(1, -1, 0)$ denoted by '$\circ$' to the desired position $(0, 0, 0)$ denoted by '$\star$' in Fig. 3.

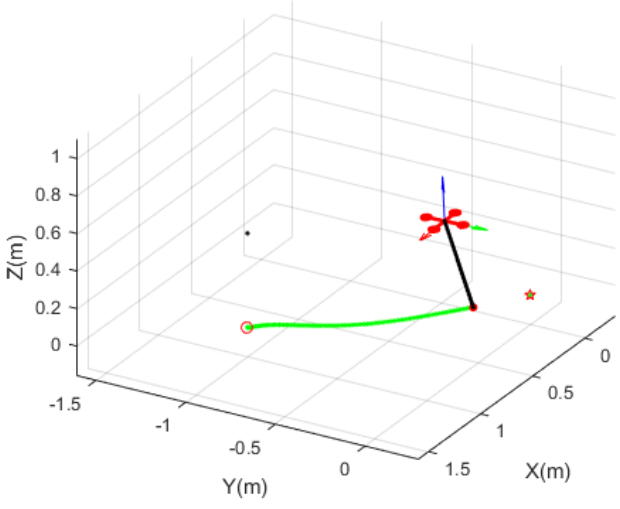

Fig. 3. Snapshot of the transporting animation

The whole simulation lasts for 10 seconds and there is an extra ΔF_z added around 4s as the disturbance. The simulation results are seen in Fig. 4-6.

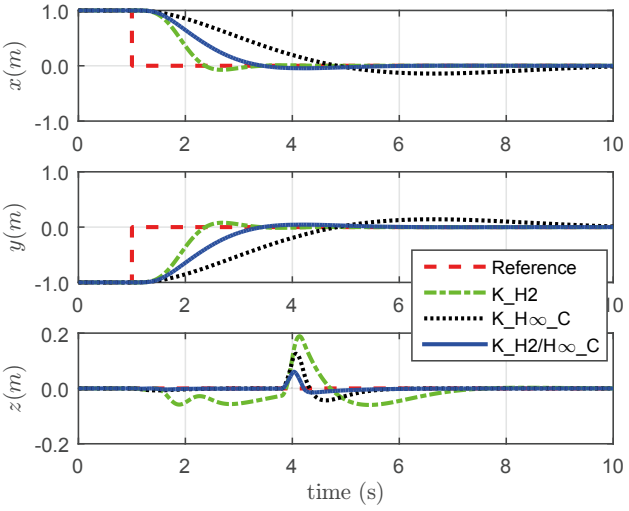

Fig. 4. Position of the payload

Fig. 4 shows the tracking position of different control strategies. H_2 controller is assigned with appropriate weight matrices for tracking errors $\boldsymbol{C}_2$ and control inputs $\boldsymbol{D}_2$. It has the shortest transportation time as well as the most aggressive swing angles. Meanwhile, H_2 has the worst robustness comparing with the other controllers when extra disturbance (ΔF_z) is added at 4s.

With extra constraints (u_{max}) for α and β, H_∞ controller has the minimum swing angles (seen Fig. 5) at the cost of the longest transportation time (seen Fig. 4).

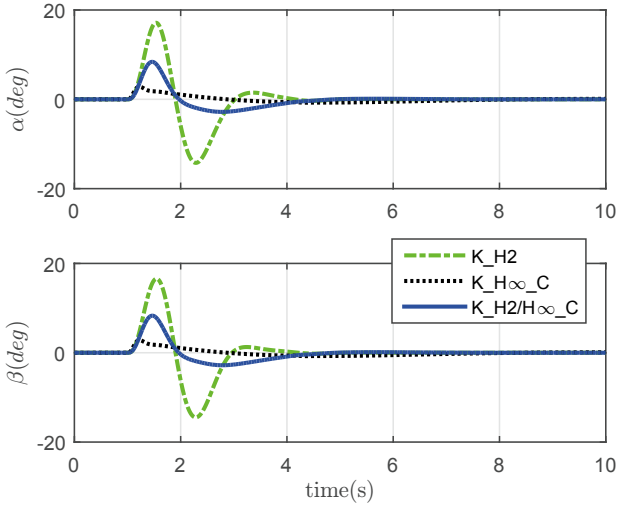

Fig. 5. Swing angles of the cable

In terms of the quadcopter's attitude (Fig. 6), H_∞ has a dramatically large rotational velocity at the start point even though its swing angle is very small. In comparison, the velocity of H_2 is smaller than H_∞ but its attitude is still very large both at the start and end point as it has the most aggressive swing angle.

The H_{mix} controller has a median transportation time and the best robustness as seen in Fig. 4. Meanwhile, it has the median swing angle and the smoothest attitude seen in Fig. 5 and Fig. 6.

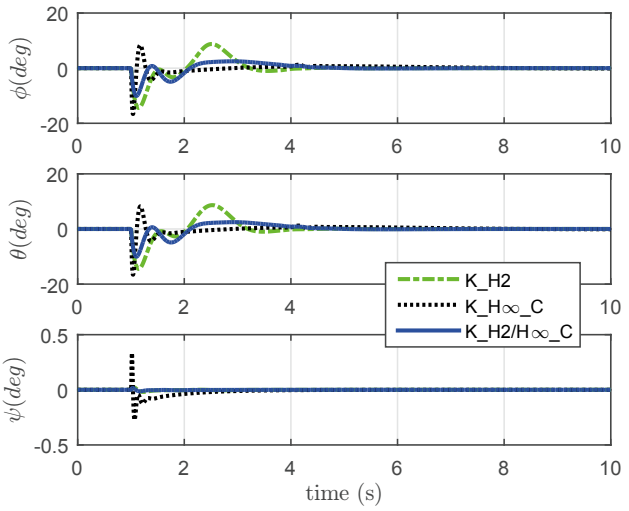

Fig. 6. Attitude of the quadcopter

Obviously, by mixing the previous two controllers H_{mix} controller keeps a good balance in increasing the transportation speed and limiting the aggressiveness for the swing angle as well as increasing the robustness.

Apart from the step response test, another simulation video for controlling the payload to track a star shape trajectory is available at `https://www.youtube.com/watch?v=zpD9ROTo-2Y\&feature=youtu.be`.

In conclusion, it is in contradiction that trying to both increase the ability to track desired trajectory and keep a less aggressive swing angle. Basically, the proposed H_{mix} method utilizes H_∞ with constraints to limit the aggressiveness of the swing angle and H_2 for a smooth attitude regulation and position tracking. The results have been validated in the simulation test.

5. CONCLUSION

This paper presents a mixed H_2/H_∞ controller with constraints for single quadcopter with a cable-suspended payload. The simulation results show that the proposed controller efficiently eliminates the position error and still keeps a smooth change for the quadcopter's attitude. At the same time, extra constraints are added to limit the aggressiveness of the swing angle. The future work is to utilize this approach for payload transportation issue with two quadcopters.

REFERENCES

Alothman, Y., Jasim, W., and Gu, D. (2015). Quadrotor lifting-transporting cable-suspended payloads control. In *Automation and Computing (ICAC), 2015 21st International Conference on*, 1–6. IEEE.

Apkarian, P., Tuan, H.D., and Bernussou, J. (2001). Continuous-time analysis, eigenstructure assignment, and $H2$ synthesis with enhanced linear matrix inequalities (LMI) characterizations. *IEEE Transactions on Automatic Control*, 46(12), 1941–1946.

Cruz, P. and Fierro, R. (2014). Autonomous lift of a cable-suspended load by an unmanned aerial robot. In *2014*

IEEE Conference on Control Applications (CCA), 802–807. IEEE.

De Crousaz, C., Farshidian, F., and Buchli, J. (2014). Aggressive optimal control for agile flight with a slung load. In *IROS 2014 Workshop on Machine Learning in Planning and Control of Robot Motion*. Citeseer.

Faust, A., Palunko, I., Cruz, P., Fierro, R., and Tapia, L. (2013). Learning swing-free trajectories for uavs with a suspended load. In *Robotics and Automation (ICRA), 2013 IEEE International Conference on*, 4902–4909. IEEE.

Filasova, A. et al. (2016). On enhanced mixed $H2/H\infty$ design conditions for control of linear time-invariant systems. In *Carpathian Control Conference (ICCC), 2016 17th International*, 384–389. IEEE.

Nonami, K. and Sivrioglu, S. (1996). Active vibration control using LMI-based mixed $H2/H\infty$ state and output feedback control with nonlinearity. In *Decision and Control, 1996., Proceedings of the 35th IEEE Conference on*, volume 1, 161–166. IEEE.

Palunko, I., Fierro, R., and Cruz, P. (2012). Trajectory generation for swing-free maneuvers of a quadrotor with suspended payload: A dynamic programming approach. In *Robotics and Automation (ICRA), 2012 IEEE International Conference on*, 2691–2697. IEEE.

Sreenath, K. and Kumar, V. (2013). Dynamics, control and planning for cooperative manipulation of payloads suspended by cables from multiple quadrotor robots. In *Robotics: Science and Systems (RSS)*.

Sreenath, K., Lee, T., and Kumar, V. (2013). Geometric control and differential flatness of a quadrotor uav with a cable-suspended load. In *52nd IEEE Conference on Decision and Control*, 2269–2274. IEEE.

Zhai, G., Murao, S., Koyama, N., and Yoshida, M. (2003). Low order $H\infty$ controller design: An lmi approach. In *European Control Conference (ECC), 2003*, 3070–3075. IEEE.

Appendix A. SOME RESULTS

Generalized forces:

$$\begin{aligned}
Q_1 &= F_z(C[\phi]C[\psi]S[\theta] + S[\phi]S[\psi]) \\
Q_2 &= F_z(-C[\psi]S[\phi] + C[\phi]S[\theta]S[\psi]) \\
Q_3 &= F_zC[\theta]C[\phi] \\
Q_4 &= F_zL_rC[\beta](C[\alpha]C[\theta]C[\phi] + S[\alpha](-C[\psi]S[\phi] + C[\phi]S[\theta]S[\psi])) \\
Q_5 &= F_zL_r(-C[\theta]C[\phi]S[\alpha]S[\beta] + C[\alpha]S[\beta](-C[\psi]S[\phi] \\
&\quad + C[\phi]S[\theta]S[\psi]) - C[\beta](C[\phi]C[\psi]S[\theta] + S[\phi]S[\psi])) \\
Q_6 &= M_x \\
Q_7 &= M_yC[\phi] - M_zS[\phi] \\
Q_8 &= -M_xS[\theta] + C[\theta](M_zC[\phi] + M_yS[\phi])
\end{aligned} \tag{A.1}$$

hereafter, C stands for cos, S stands for sin.

Matrix M:

$$\boldsymbol{M} = \begin{bmatrix} \boldsymbol{M}_{11} & \boldsymbol{0}_{5\times3} \\ \boldsymbol{0}_{3\times5} & \boldsymbol{M}_{22} \end{bmatrix} \tag{A.2}$$

where, $\boldsymbol{M}_{11}$ and $\boldsymbol{M}_{22}$ are defined as follows:

$$\boldsymbol{M}_{11} = \begin{bmatrix} m_P+m_Q & 0 & 0 & 0 & -L_rm_QC\beta \\ 0 & m_P+m_Q & 0 & L_rm_QC\beta S\alpha & L_rm_QC\alpha S\beta \\ 0 & 0 & m_P+m_Q & L_rm_QC\alpha C\beta & -L_rm_QS\alpha S\beta \\ 0 & L_rm_QC\beta S\alpha & L_rm_QC\alpha C\beta & L_r^2m_QC\beta^2 & 0 \\ -L_rm_QC\beta & L_rm_QC\alpha S\beta & -L_rm_QS\alpha S\beta & 0 & L_r^2m_Q \end{bmatrix}$$

$$\boldsymbol{M}_{22} = \begin{bmatrix} I_x & 0 & -I_xS\theta \\ 0 & I_yC^2\phi + I_zS^2\phi & (I_y-I_z)C\theta C\phi S\phi \\ -I_xS\theta & (I_y-I_z)C\theta C\phi S\phi & I_xS^2\theta + C^2\theta(I_zC^2\phi + I_yS^2\phi) \end{bmatrix}$$

Definitions of function $f(\boldsymbol{x}, \boldsymbol{u})$:

$$\begin{aligned}
f_1(\boldsymbol{x},\boldsymbol{u}) &= F_zC[\phi]C[\psi]S[\theta] + F_zS[\phi]S[\psi] - L_rm_QS[\beta]\dot{\beta}^2 \\
f_2(\boldsymbol{x},\boldsymbol{u}) &= -F_zC[\psi]S[\phi] + F_zC[\phi]S[\theta]S[\psi] \\
&\quad + L_rm_Q\left(2S[\alpha]S[\beta]\dot{\alpha}\dot{\beta} - C[\alpha]C[\beta]\left(\dot{\alpha}^2+\dot{\beta}^2\right)\right) \\
f_3(\boldsymbol{x},\boldsymbol{u}) &= -g(m_P+m_Q) + F_zC[\theta]C[\phi] \\
&\quad + L_rm_Q\left(2C[\alpha]S[\beta]\dot{\alpha}\dot{\beta} + C[\beta]S[\alpha]\left(\dot{\alpha}^2+\dot{\beta}^2\right)\right) \\
f_4(\boldsymbol{x},\boldsymbol{u}) &= L_rC[\beta](C[\alpha](-gm_Q + F_zC[\theta]C[\phi]) \\
&\quad + F_zS[\alpha](-C[\psi]S[\phi] + C[\phi]S[\theta]S[\psi]) + 2L_rm_QS[\beta]\dot{\alpha}\dot{\beta}) \\
f_5(\boldsymbol{x},\boldsymbol{u}) &= -L_r((-gm_Q + F_zC[\theta]C[\phi])S[\alpha]S[\beta] \\
&\quad + F_z(C[\alpha]S[\beta](C[\psi]S[\phi] - C[\phi]S[\theta]S[\psi]) \\
&\quad + C[\beta](C[\phi]C[\psi]S[\theta] + S[\phi]S[\psi])) + L_rm_QC[\beta]S[\beta]\dot{\alpha}^2) \\
f_6(\boldsymbol{x},\boldsymbol{u}) &= M_x + (-I_y+I_z)C[\phi]S[\phi]\dot{\theta}^2 + C[\theta](I_x + (I_y-I_z)C[2\phi])\dot{\theta}\dot{\psi} \\
&\quad + (I_y-I_z)C^2[\theta]C[\phi]S[\phi]\dot{\psi}^2 \\
f_7(\boldsymbol{x},\boldsymbol{u}) &= M_yC[\phi] - M_zS[\phi] + (I_y-I_z)S[2\phi]\dot{\theta}\dot{\phi} \\
&\quad + C[\theta]\dot{\psi}\left(-(I_x + (I_y-I_z)C[2\phi])\dot{\phi} + S[\theta]\left(I_x - I_zC^2[\phi] - I_yS^2[\phi]\right)\dot{\psi}\right) \\
f_8(\boldsymbol{x},\boldsymbol{u}) &= -M_xS[\theta] + C[\theta](M_zC[\phi] + M_yS[\phi]) \\
&\quad + (I_y-I_z)C[\phi]S[\theta]S[\phi]\dot{\theta}^2 + (-I_y+I_z)C[\theta]^2S[2\phi]\dot{\phi}\dot{\psi} \\
&\quad + \dot{\theta}\left(C[\theta](I_x + (-I_y+I_z)C[2\phi])\dot{\phi} + S[2\theta]\left(-I_x + I_zC^2[\phi] + I_yS^2[\phi]\right)\dot{\psi}\right)
\end{aligned} \tag{A.3}$$

Linearized model:

$$\boldsymbol{A} = \begin{pmatrix}
0 & 1.0 & 0 & 0 & 0 & 0 & 0 & 0 & 0 & 0 & 0 & 0 & 0 & 0 & 0 \\
0 & 0 & 0 & 0 & 0 & 0 & 0 & 0 & 0.8909 & 0 & 0 & 0 & 10.6909 & 0 & 0 & 0 \\
0 & 0 & 0 & 1.0 & 0 & 0 & 0 & 0 & 0 & 0 & 0 & 0 & 0 & 0 & 0 & 0 \\
0 & 0 & 0 & 0 & 0 & 0 & -0.8909 & 0 & 0 & 0 & -10.6909 & 0 & 0 & 0 & 0 & 0 \\
0 & 0 & 0 & 0 & 0 & 1.0 & 0 & 0 & 0 & 0 & 0 & 0 & 0 & 0 & 0 & 0 \\
0 & 0 & 0 & 0 & 0 & 0 & 0 & 0 & 0 & 0 & 0 & 0 & 0 & 0 & 0 & 0 \\
0 & 0 & 0 & 0 & 0 & 0 & 0 & 1.0 & 0 & 0 & 0 & 0 & 0 & 0 & 0 & 0 \\
0 & 0 & 0 & 0 & 0 & 0 & -21.3818 & 0 & 0 & 0 & -21.3818 & 0 & 0 & 0 & 0 & 0 \\
0 & 0 & 0 & 0 & 0 & 0 & 0 & 0 & 0 & 1.0 & 0 & 0 & 0 & 0 & 0 & 0 \\
0 & 0 & 0 & 0 & 0 & 0 & 0 & 0 & -21.0 & 0 & 0 & 0 & -21.3818 & 0 & 0 & 0 \\
0 & 0 & 0 & 0 & 0 & 0 & 0 & 0 & 0 & 0 & 0 & 1.0 & 0 & 0 & 0 & 0 \\
0 & 0 & 0 & 0 & 0 & 0 & 0 & 0 & 0 & 0 & 0 & 0 & 0 & 0 & 0 & 0 \\
0 & 0 & 0 & 0 & 0 & 0 & 0 & 0 & 0 & 0 & 0 & 0 & 0 & 1.0 & 0 & 0 \\
0 & 0 & 0 & 0 & 0 & 0 & 0 & 0 & 0 & 0 & 0 & 0 & 0 & 0 & 0 & 0 \\
0 & 0 & 0 & 0 & 0 & 0 & 0 & 0 & 0 & 0 & 0 & 0 & 0 & 0 & 0 & 1.0 \\
0 & 0 & 0 & 0 & 0 & 0 & 0 & 0 & 0 & 0 & 0 & 0 & 0 & 0 & 0 & 0
\end{pmatrix} \tag{A.4}$$

$$\boldsymbol{B} = \begin{pmatrix}
0 & 0 & 0 & 0 \\
0 & 0 & 0 & 0 \\
0 & 0 & 0 & 0 \\
0 & 0 & 0 & 0 \\
0 & 0 & 0 & 0 \\
1.6667 & 0 & 0 & 0 \\
0 & 0 & 0 & 0 \\
0 & 0 & 0 & 0 \\
0 & 0 & 0 & 0 \\
0 & 0 & 0 & 0 \\
0 & 0 & 0 & 0 \\
0 & 434.7826 & 0 & 0 \\
0 & 0 & 0 & 0 \\
0 & 0 & 357.1429 & 0 \\
0 & 0 & 0 & 0 \\
0 & 0 & 0 & 217.3913
\end{pmatrix} \tag{A.5}$$